Electronic Supplementary Material (ESI) for Nanoscale.

SUPPORTING INFROMATION

Solution and interfacial self-assembly of *Bacillus subtilis* bacterial lipoteichoic acid (LTA): Nanoclustering, and effects of Ca^{2+} and temperature

Bhavesh Bharatiya, [a] Magdalena Wlodek, [b] Robert Harniman, [a] Ralf Schweins, [c]

Judith Mantell, [d] Gang Wang, [a] Piotr Warszynski, [b] Wuge H. Briscoe [a*]

[a] School of Chemistry, University of Bristol, Cantock's Close, Bristol BS8 1TS, United Kingdom

[b] Jerzy Haber Institute of Catalysis and Surface Chemistry, Polish Academy of Sciences, Niezapominajek 8, PL-30239 Krakow, Poland

[c] Institut Laue-Langevin, DS/LSS, 71 Avenue des Martyrs, Grenoble 38000, France

[d] Wolfson Bioimaging Facility, University of Bristol, Medical Sciences Building, University Walk, Bristol BS8 1TD, United Kingdom

Corresponding author: E-mail - wuge.briscoe@bristol.ac.uk; Phone - +44 (0)117 3318256

S1. SANS intensity profiles as a function of LTA concentration at different temperatures

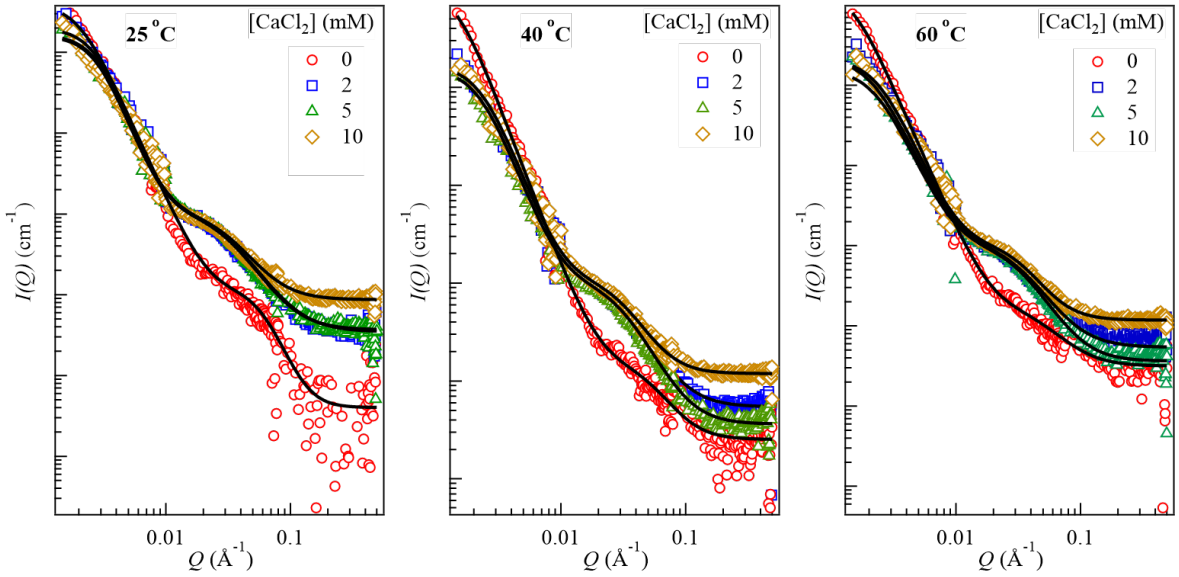

Figure S1(a). SANS scattering intensity *I* vs *Q* profiles showing change in the absolute intensities for 2 mg mL^{-1} LTA aggregates containing 0 – 10 mM $CaCl_2$ at 25, 40 and 60 °C. Symbols are the data points and the solid lines represent the best fits using the *two-Lorentzian* model.

The absolute SANS intensity profiles for the change in the LTA aggregate size on $CaCl_2$ addition at different temperatures are shown in **Figure S1(a)**. The scattering intensity decreased with corresponding increase in the $CaCl_2$ concentration up to 5 mM and remains relatively constant at 10 mM.

The fitting of these scattering data was attempted using several models. We have trialled fitting the SANS data with shape-dependent models, such as sphere, core-shell sphere, core-shell ellipsoid, and triaxial ellipsoid models (**cf. Figure S1(b-e) below**). However, due to the polydisperse nature of the aggregates, the fitting was not satisfactory. Furthermore, we have also trialled fitting the SANS data in different *q* ranges using different models (cf. **Figure S1(b-e) below**), with some the partial fitting generating good χ^2 values in limited *q*-ranges but not over the whole *q*-range. For instance, the low-*q* data could be well described by the fractal model, whilst the high-*q* data by the correlation length model, as shown below. In the main text of this ms, we have focused on discussing the two Lorentzian model as it allowed fitting of

the SANS data in both low-*q* and high-*q* regimes simultaneously. We summarise some of the models that have been attempted but did not provide fully sufficient and physically feasible descriptions of the LTA aggregates in aqueous solutions.

1. G*el-fit (Low-Q)*

Here, the scattering intensity is described by the following equation:

$$I(Q) = I(0)_L \frac{1}{(1+[((D+1/3)Q^2 a_1^2)]^{D/2}} + I(0)_G exp(-Q^2 a_2^2) + B \;\ldots\ldots \boldsymbol{eq.(S1)}$$

where $a_2^2 \approx \frac{R_g^2}{3}$. Here, a_1 and a_2 correspond to the two characteristic length scales in the gel system, with a_1 the shorter and a_2 the longer length scales; and R_g is the radius of gyration.

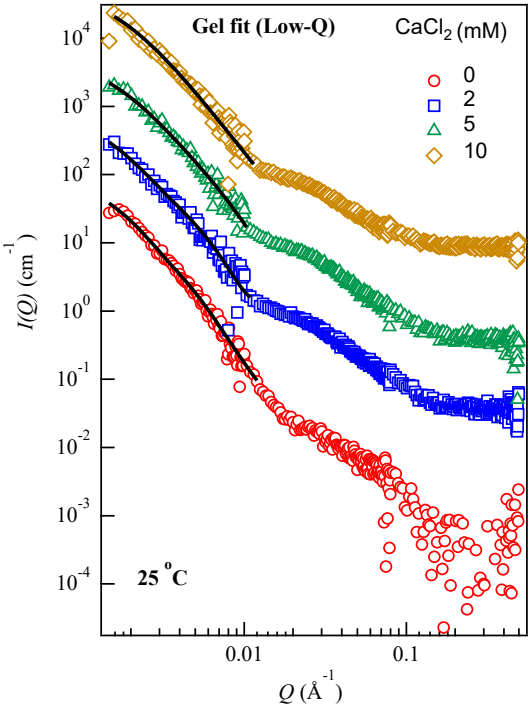

Figure S1(b). SANS intensity *I* vs *Q* profiles for 2 mg mL^{-1} LTA aqueous solutions containing 0 – 10 mM $CaCl_2$ at 25, 40 and 60 °C. Symbols are the data points and solid lines represent the best fits using the *gel fit* in low-Q region of the spectra. For clarity, the SANS profiles are scaled on the *y*-axis. The plots for 2,5 and 10 mM $CaCl_2$ cases are shown with a Y-axis multiplication factor of 10, 100 and 1000, respectively.

Table S1(a): Fitted SANS parameters for 2 mg mL^{-1} LTA aqueous solutions at 25 °C. Here, χ^2 indicates the goodness of the fit.

$[Ca^{2+}]$, mM	Guinier scale	Lorentz scale	R_g(Å)	Fractal dimension	Correlation length, Å	χ^2
0	-2.66 ± 15000	22.60 ± 15400	747.3 ± 60.5	3.90 ± 0.34	420.65 ± 79.3	0.9
2	0.74 ± 11397	22.15±3412	357.53 ±- 23.69	4.10 ± 2.01	481.13 ± 365.1	1.5
5	0.21 ± 28202	24.82 ± 32839000	296.74 ± 154.44	3.18 ± 0.55	526.29 ± 197.9	0.8
10	1.06 ± 28049	37.86 ± 9989	1490.2 ± 13694	3.07 +- 0.53	509.76 ± 377	0.9

Conclusion: *Fitting gave physically irrelevant parameters.*

2. *Sphere (High-Q)*

$$I(q) = \frac{scale}{V} \cdot \left[3V(\Delta\rho).\frac{sin(qr) - qr\,cos(qr))}{qr^3}\right]^2 + Background \quad \ldots\ldots\ldots \boldsymbol{eq.(S2)}$$

where *scale* is a volume fraction, *V* is the volume of the scatterer, *r* is the radius of the sphere and background is the background level. $\Delta\rho$ is the difference in scattering length densities (SLDs) of the scatterer and the solvent.

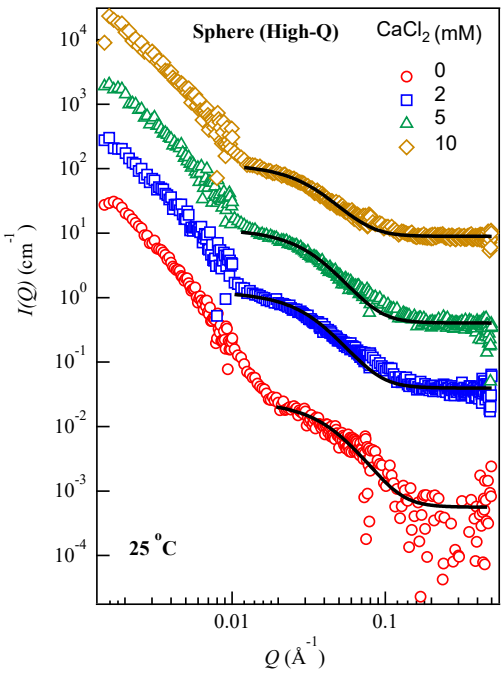

Figure S1(c). SANS intensity *I* vs *Q* profiles for 2 mg mL^{-1} LTA aqueous solutions containing 0 – 10 mM $CaCl_2$ at 25, 40 and 60 °C. Symbols are the data points and solid lines represent the best fits using the

sphere model in High-Q region of the spectra. For clarity, the SANS profiles are scaled on the *y*-axis. The plots for 2,5 and 10 mM $CaCl_2$ cases are shown with a Y-axis multiplication factor of 10, 100 and 1000, respectively.

Table S1(b): Fitted SANS parameters for 2 mg mL^{-1} LTA aqueous solutions at 25 °C. Here, χ^2 indicates the goodness of the fit.

$[Ca^{2+}]$, mM	radius, Å	Volume fraction	χ^2
0	17.90 ± 0.4	3.98 e-05 ± 1.7 e-06	5.6
2	21.58 ± 2.8	2.94 e-05 ± 1.7 e-06	4.9
5	22.37 ± 0.1	8.79 e-05 ± 9.9 e-06	3.3
10	22.10 ± 0.1	8.75 e-05 ± 1.0 e-06	2.7

Conclusion: *Fitting with physically irrelevant parameters.*

3. *Lorentz (High-Q)*

$$I(q) = \frac{scale}{1 + (qL)^2} + Background \ldots\ldots\ldots \boldsymbol{eq.(S3)}$$

where *L* is the correlation length.

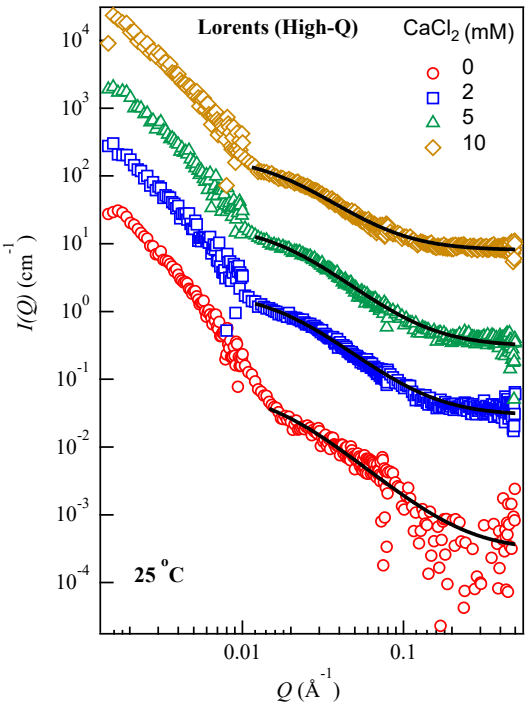

Figure S1(d). SANS intensity *I* vs *Q* profiles for 2 mg mL^{-1} LTA aqueous solutions containing 0 – 10 mM $CaCl_2$ at 25, 40 and 60 °C. Symbols are the data points and solid lines represent the best fits using the

Lorentz model in High-Q region of the spectra. For clarity, the SANS profiles are scaled on the *y*-axis. The plots for 2,5 and 10 mM $CaCl_2$ cases are shown with a Y-axis multiplication factor of 10, 100 and 1000, respectively.

Table S1(c): Fitted SANS parameters for 2 mg mL^{-1} LTA aqueous solutions at 25 °C. Here, χ^2 indicates the goodness of the fit.

$[Ca^{2+}]$, mM	Scale	Correlation length Å	χ^2
0	0.07 ± 0.004	64.11 ± 3.01	2.1
2	0.19 ± 0.003	58.18 ± 0.74	1.6
5	0.18 ± 0.003	58.74 ± 0.78	1.8
10	0.18 ± 0.003	59.24 ± 0.78	1.8

Figure S1(d) shows the SANS scattering plots for 2 mg mL^{-1} LTA aqueous solutions at 25 °C in the presence of different calcium chloride concentrations (0-10 mM). The scattering curve demonstrated two distinct slopes and the curve is very well fitted by the Lorentz model in the high-Q region (0.02-0.49 $Å^{-1}$). The obtained fitting parameters indicate a marginal decrease in the correlation length values with addition of calcium chloride. The value around ~ 60 Å describes the length scales corresponding to the average distances between the entanglement points. As shown in Figure 2 in the manuscript, the hydrophilic polyglycerol chains possess coiled morphology, and the calcium addition decreases the average distances corresponding to intra- and inter-micellar entanglement points, formed mainly due to the H-bonding and calcium ion bridges.

4. *Mass fractal*

$$I(q) = scale \times P(q)\,S(q) + background \quad \ldots\ldots \boldsymbol{eq.S4(a)}$$

$$P(q) = F(qR)^2 \quad \ldots\ldots \boldsymbol{eq.4(b)}$$

$$S(q) = \frac{\Gamma(D_m - 1)\zeta^{(D_m - 1)}}{[1 + (q\zeta)^2]^{(D_m - 1)/2}} \frac{sin\,[(D_m - 1)\,tan^{-1}(q\,\zeta)}{q} \quad \ldots\ldots \boldsymbol{eq.S4(c)}$$

$$scale = scale\_factor \times NV^2(\rho_{particle} - \rho_{solvent})^2 \ldots\ldots \boldsymbol{eq.S4(d)}$$

$$V = 4/3\,\pi R^3 \ldots\ldots \boldsymbol{eq.S4(e)}$$

Here, R is the radius of the building block, D_m is the mass fractal dimension, ζ is the cut-off length, $\rho_{solvent}$ is the scattering length density of the solvent, and $\rho_{particle}$ is the scattering length density of particles.

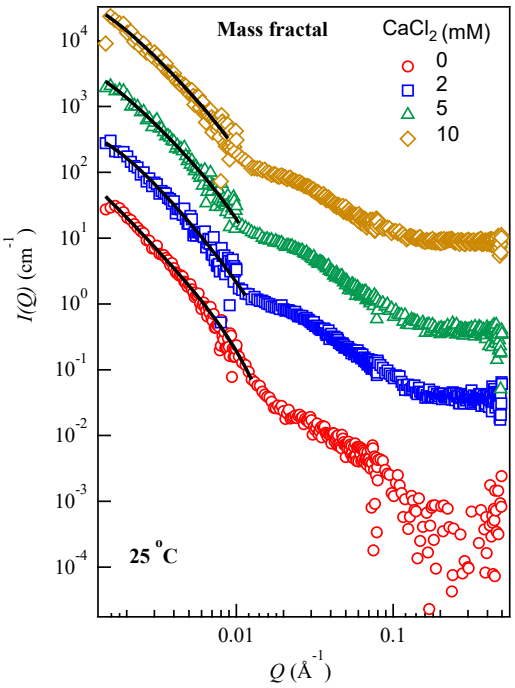

Figure S1(e). SANS intensity *I* vs *Q* profiles for 2 mg mL^{-1} LTA aqueous solutions containing 0 – 10 mM $CaCl_2$ at 25, 40 and 60 °C. Symbols are the data points and solid lines represent the best fits using the *mass fractal* model in the low-Q region of the spectra. For clarity, the SANS profiles are scaled on the *y*-axis. The plots for 2,5 and 10 mM $CaCl_2$ cases are shown with a Y-axis multiplication factor of 10, 100 and 1000, respectively.

Table S1(d): Fitted SANS parameters for 2 mg mL^{-1} LTA aqueous solutions at 25 ^{o}C. Here, χ^2 indicates the goodness of the fit.

$[Ca^{2+}]$, mM	radius, Å	Fractal dimension	scale	χ^2
0	204.62 ± 01.63	2.36 ± 0.002	1.062e-05	1.2
2	168.07 ± 17.23	2.33 ± 0.007	1.063e-05	0.8
5	176.77 ± 04.19	2.30 ± 0.003	1.066e-05	0.8
10	159.07 ± 16.49	2.31 ± 0.004	1.063e-05	1.3

Figure S1(e) shows the SANS scattering plots for 2 mg mL^{-1} LTA aqueous solutions at 25 ^{o}C in the presence of different calcium chloride concentrations (0-10 mM). The scattering curve demonstrated two distinct slopes and the curve is very well fitted by the mass-fractal model in the low-Q region (0.0015-0.018 $Å^{-1}$). The fitted radius values for the LTA micelles decrease with corresponding addition of calcium chloride. The initial value ~ 204 Å decreases to ~159 Å in the presence of 10 mM $CaCl_2$. The calcium bridges reduced the micellar size by decreasing the H-bonding of hydrophilic chains with water. This shrinking is indicative of decreased water-polymer interactions. The fractal values ~ 2.3 indicated strong water-polymer chain interactions, which is understood by the presence of -OH and ionic PO_4^{-3} groups in the polyglycerolphopshate chains. The scale values in the order of 10^{-5} indicate a very low value of the volume fraction, which is understood by the considerably dilute LTA concentration of 2 mg mL^{-1}.

<u>Other models attempted</u>:

- Core-shell sphere: Fitting did not converge
- Core-shell ellipsoid: Fitting did not converge
- Triaxial ellipsoid: Fitting did not converge
- Fractal (shape independent): Fitting did not converge

- Guinier fitting: No valid Guinier Region present
- Sphere-Mass fractal combined model: Fitting did not converge
- Lorentz-Mass fractal combined model: Fitting did not converge

S2. LTA aggregates adsorbed at the mica-water interface:

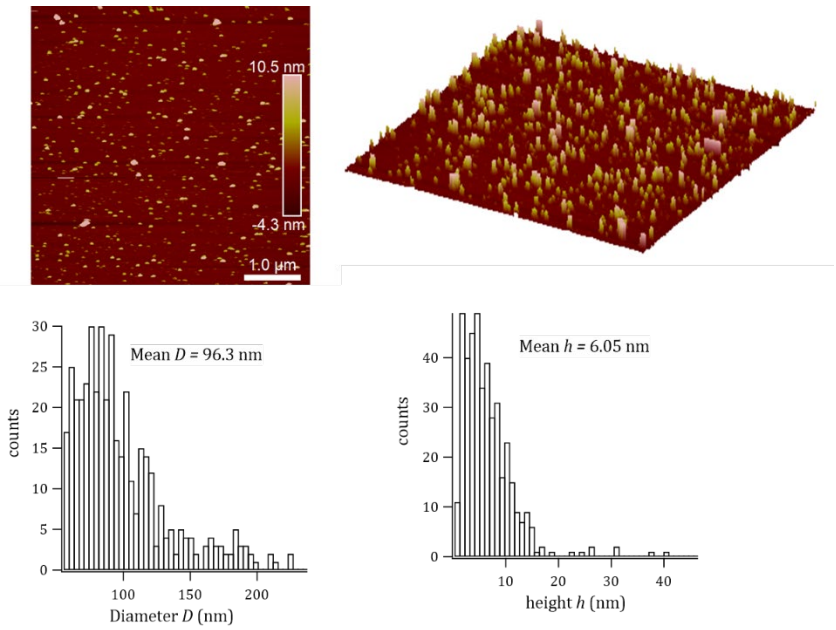

Figure S2(a). AFM images showing the topography the mica-water interface in 2 mg mL^{-1} LTA in the presence of 10 mM $CaCl_2$ at 25 ^{o}C, along with the histograms showing the particle diameter and height distribution on the surface.

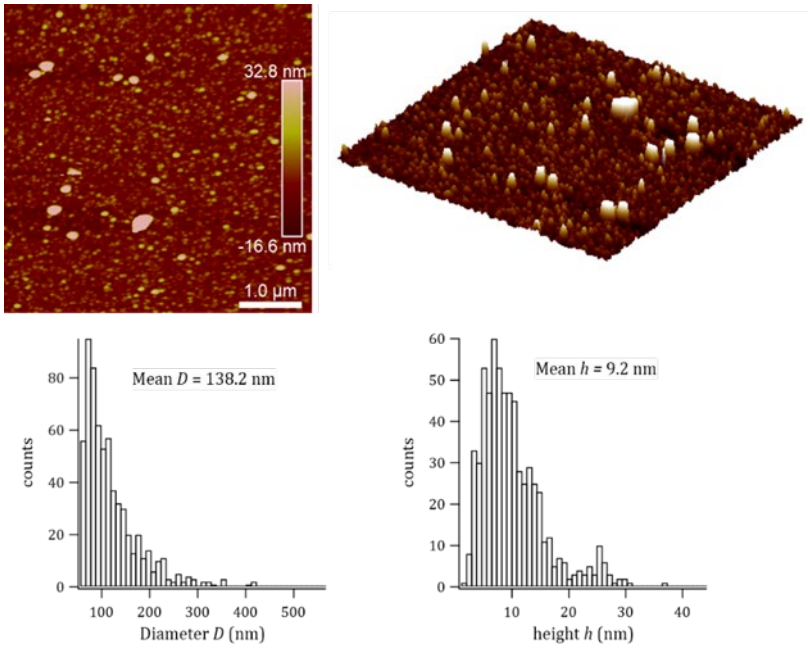

Figure S2(b). The AFM images showing the topography the mica-water interface in 2 mg mL^{-1} LTA in the presence of 10 mM $CaCl_2$ at 40 °C, along with the histograms showing the particle diameter and height distribution on the surface.

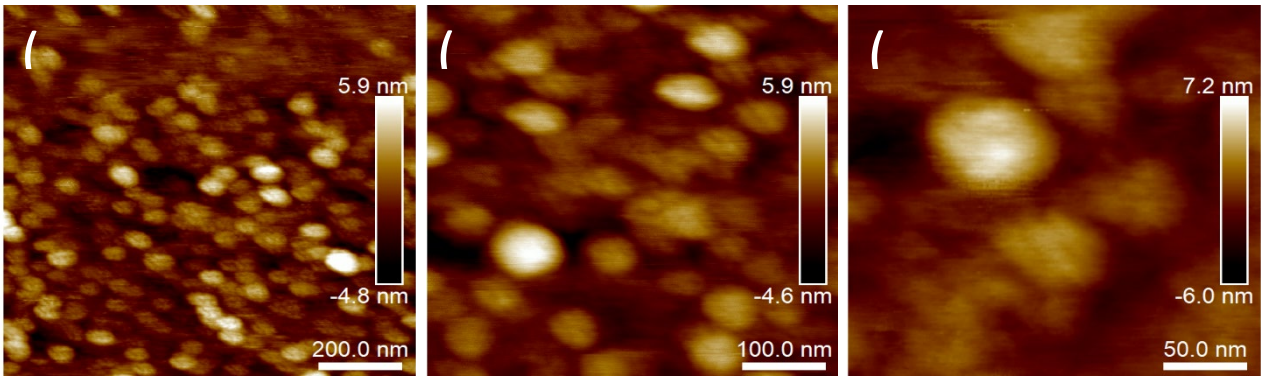

Figure S2(c). AFM images showing the raspberry aggregate feature (cf. Fig. 6B in the main text) on different scan sizes: (A) 1 μm x 1 μm, (B) 500 nm x 500 nm, and (C) 200 nm x 200 nm. The images were collected for 2 mg mL^{-1} LTA aggregates adsorbed in the presence of 10 mM $CaCl_2$ at the mica-water interface at 25 °C.

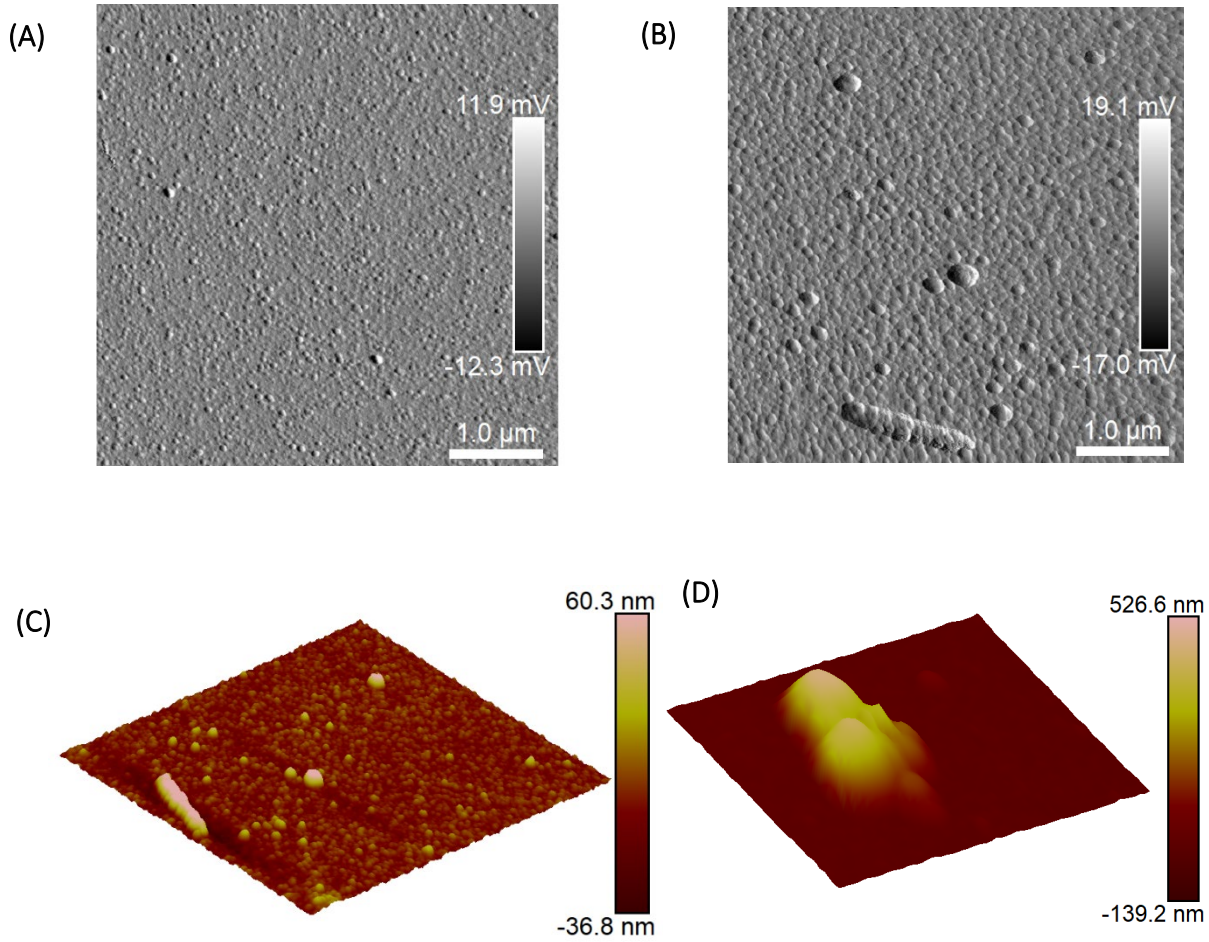

Figure S2(d). AFM images showing the aggregate topography at the mica-water interface in 2 mg mL^{-1} LTA solution in the presence of 10 mM $CaCl_2$ at 40 °C. (A) and (B): The error signals corresponding to Fig.6A and D in the main text. 3D surfaces of Fig. 6D (C) and another example of a larger aggregate at 40 °C (D).

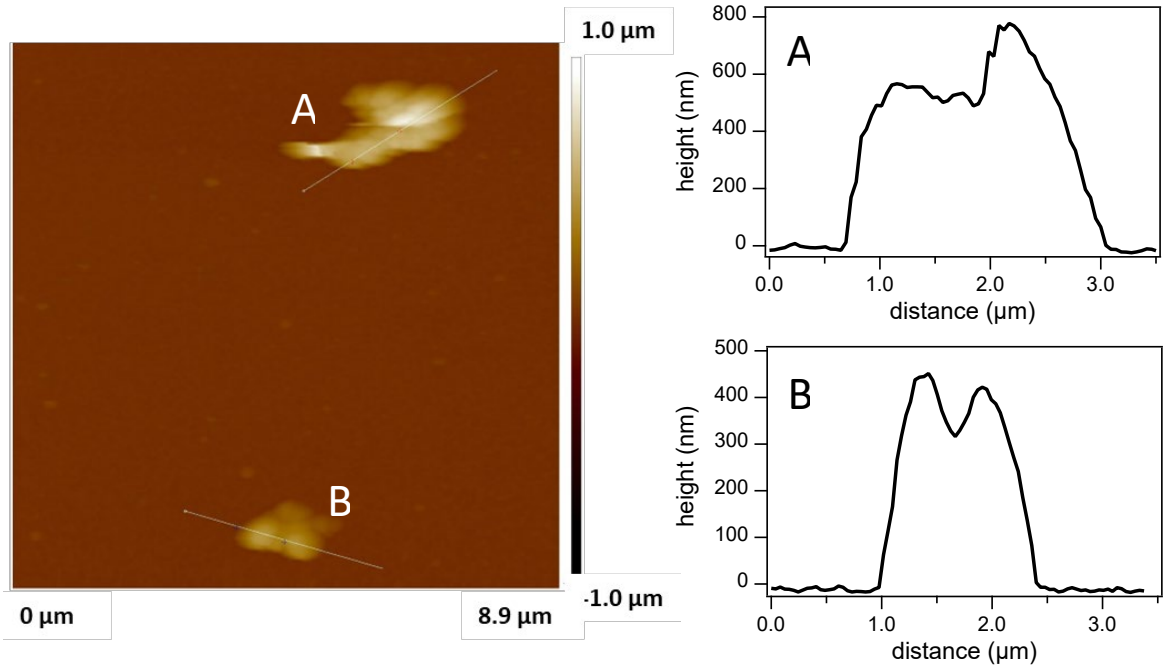

Figure S2(e). An AFM image showing two large aggregates at the mica-water interface in 2 mg mL^{-1} LTA solution in the presence of 10 mM $CaCl_2$ at 40 °C, with the line profiles for aggregates labelled A and B on the right-hand side.